Preparation and Inoculation of BMCs

Bone marrow cells were collected from the femurs and tibias of BALB/c mice. In brief, Donor BMCs from female BALB/c mice were flushed from tibiae, femurs, and humeri using Roswell Park Memorial Institute (RPMI) 1640 medium (Niken CM1101, Japan) supplemented with 2% heat-inactivated fetal calf serum (PAA.A15–001; Austria) on ice. BMCs were filtered through a sterile nylon mesh, resuspended in sterile phosphate-buffered saline. IBM-BMT injection was carried out according to the method described previously (*9*). In brief, the knee was flexed to 90 degrees and the proximal side of the tibia was drawn to the anterior. A 26-gauge needle was inserted into the joint surface of the left tibia through the patellar tendon and then inserted into the bone marrow (BM) cavity of the left tibia. Using a microsyringe (50 μL; Hamilton Company, Reno, NV), the donor BMCs (1×10^7/10 μL/mouse) were injected into the BM cavity.

Flow Cytometry

BMCs, spleen cells, and peripheral blood cells were prepared from the recipient mice after three months with bone marrow transplantation, followed by red blood cell lysis with ammonium chloride (8.3 g/ml; Sigma-Aldrich, St. Louis, MO). To detect donor- or residual recipient-derived cells, the cells were stained with fluorescein isothiocyanate (FITC)–conjugated anti–H-$2K^d$ and phycoerythrin (PE)–conjugated anti-H-$2K^b$ monoclonal antibodies (mAbs; PharMingen, San Diego, CA). The cells were analyzed using a FACScan (Becton, Dickinson and Company, Mountain View, CA).

Mixed Leukocyte Reaction

Mixed leukocyte reaction (MLR) was performed as follows: splenic T cells (derived from normal C57BL/6, BALB/c, C3H mice and OvX+IBM-BMT+OT mice) were isolated by mechanical dissociation using microscope slides followed by red blood cell lysis with ammonium chloride (8.3 g/ml; Sigma-Aldrich). The 4×10^5 responder T cells were cultured with 4×10^5 or 3×10^5 irradiated (15 Gy) stimulator spleen cells for 96 hr in 10% FBS RPMI with 50 μM 2-ME, then pulsed with 0.5 μCi of [^{3}H]-thymidine for the last 18 hr of the culturing period.

Histology of Bone

Vertebras were fixed in 10% formalin and then decalcified and paraffin-embedded. The lumbar vertebra was sectioned to obtain a longitudinal midline section through the vertebral body, and then the sections were stained with hematoxylin and eosin (H&E). Left tibias of mice were removed the soft tissues, stored in 70% ethanol for peripheral quantitative computed tomography (pQCT) analysis. Bone histomorphometry and pQCT were used to evaluate bone mass. Percentage of trabecular bone area (B.Ar/T.Ar) was used to evaluate bone mass in histomorphometry: the fourth lumbar vertebra of every sample was cut into five consecutive sections, and these sections were measured by image analysis software (Lumina vision 1 image analysis system, Japan). A small animal pQCT (XCT Research SA, Stratec Medizjntechnik, Pforzheim, Germany) was used for the measurements. When detected, bone was fixed in plastic tube (8-mm diameter) with a spring and scanned with pQCT equipment (XCT 540; Stratec). For the measurement levels in tibia, the reference line was placed at the proximal end of the bone. Three cross-sections, at 0.3-mm intervals, were analyzed 1.8 mm from the reference line. Measurements were also taken from two sections separated by 1 mm, starting 2.5 mm above a reference line at the tibiofibular junction. Special Software version 5.40 (Stratec) was used to analyze the images of each section, with a voxel size of 0.10 mm. The total bone mineral densities (BMD) of the proximal tibia were applied for BMD analyses.

Histology of Ovary and Uterus

Three months after IBM-BMT, the uteri, and their ovary, including the allogeneic ovary transplanted under the renal capsules were removed, weighed and then fixed in 10% formalin. The sections were stained with H&E to observe ovarian and uterine morphology.

Serum Estradiol Levels

Serum specimens were collected from the treated and nontreated B6 mice, Serum samples were separated by centrifugation and stored at −80°C until used for measurements. Serum estradiol was quantified by an enzyme-linked immunosorbent assay (ELISA) kit (IBL-Hamburg GmbH Corp., Hamburg, Germany).

Urine Deoxypyridinoline (DPD) Analyses

Urine specimens were collected from the treated and nontreated B6 mice, stored at −80°C until used for measurements. The urinary DPD was quantified by an ELISA kit (Quidel Corp., San Diego, CA) to evaluate the bone loss.

Statistical Analyses

All data were presented as mean±SD. Significance of the results was determined by two-way analysis of variance. Differences were calculated by Students t test. A P value <0.01 was considered statistically significant.

RESULTS

In our preliminary experiments, we compared the survival rates of chimeric mice (BALB/c→B6) treated with conventional BMT (intravenous injection of bone marrow cells: IV-BMT) with those treated with IBM-BMT. IV-BMT-treated chimeric mice showed significantly shorter survival than IBM-BMT-treated chimeric mice, although those mice in the IV-BMT-treated group that did survive showed full chimerism (>98% donor type); we used a lethal irradiation dose (9.5 Gy) in this experiment to examine the effects of irradiation on osteoporosis and ovarian dysfunction. Therefore, in the present study (as shown in Fig. 1A), we first ovariectomized B6 mice (8 weeks old) and, 3 months later, irradiated them with 9.5 Gy. They received IBM-BMT (instead of IV-BMT) the day after the irradiation.

Cell Surface Antigens

Three months after IBM-BMT, we carried out flow cytometrical analyses using BMCs, spleen cells and peripheral blood cells obtained from the recipient mice and examined the engraftment of donor-derived cells. The percentages of

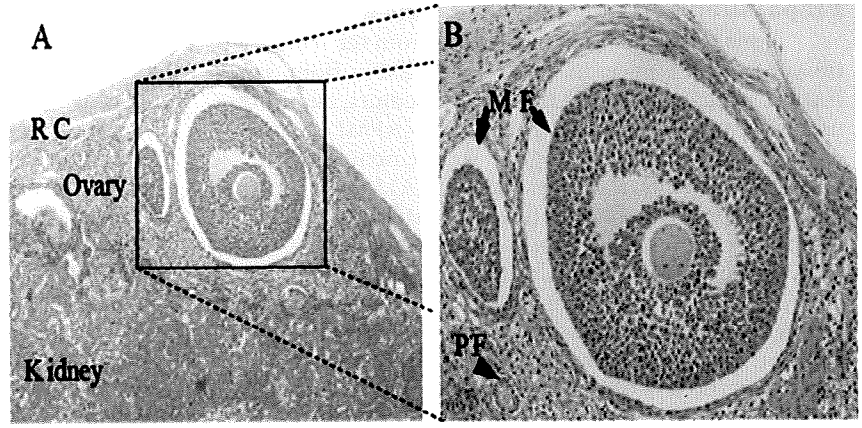

FIGURE 2. Histology of transplanted ovary after IBM-BMT. Three months after IBM-BMT and OT, the ovary was accepted (original magnification ×100, A) with a large number of mature follicles (MF) and primary follicles (PF) (original magnification×200, B) under the renal capsule (RC).

donor (BALB/c) – derived cells (H-2k^d) in the peripheral blood (Fig. 1B), BM, and spleen are 99.23%, 99.69%, and 99.54%, respectively.

Immunological Functions

We performed mixed lymphocyte reaction (MLR) using T cells as a responder obtained from the spleen of IBM-BMT-treated mice. Newly-developed T cells, as shown in Figure 1C, were tolerant of both host (C57BL/6)-type and donor (BALB/c)-type major histocompatibility complex (MHC) determinants, whereas they showed normal responses to the third-party (C3H) cells.

Histology and Weight of Ovary and Uterus

Three months after IBM-BMT+OT, the mice were sacrificed and confirmed that allogeneic ovaries had been accepted under the renal capsules of B6 mice (Fig. 2). In the mice, there were a large number of growing follicles in different stages of development, such as mature follicles, primary follicles and primordial follicles. The uteri showed normal endometrium including endometrial glands. However, in the OvX+IBM-BMT group (without OT), the uteri showed atrophic endometrium and few endometrial glands (Fig. 3A). Uterus/body weight ratios significantly increased in the OvX+IBM-BMT+OT group, compared with the OvX+IBM-BMT group or the OvX group (Fig. 3B). Uterine weight also increased in the OvX+IBM-BMT+OT group, compared with the OvX+IBM-BMT group. These results indicate that OT leads to the secretion of estrogen and restores uterine growth in the OvX mice.

Bone Histology

In the OvX+IBM-BMT+OT group, the sections of a lumbar vertebral-4 (L4) body showed that trabeculae number, thickness, and longness increased, in comparison with the OvX+IBM-BMT group, indicating that bone loss was prevented, while, in the OvX+IBM-BMT group, trabeculae were thin, and trabecular numbers decreased in comparison with the OvX group, the OvX+IBM-BMT+OT group, and the sham-operated group (Fig. 4). Histomorphometry and bone mineral densitometry were utilized to assess the bone mass of lumbar vertebrae and tibiae, respectively. The percentages of trabecular bone area (B.Ar/T.Ar) of lumbar vertebrae in the OvX+IBM-BMT+OT group increased significantly, compared with the OvX+IBM-BMT group. The total BMD of the proximal tibia are determined with pQCT. After IBM-BMT, the OT group maintained their mass, while the bone mass in the OvX+IBM-BMT group rapidly decreased; there were significant differences between the OvX group and the OvX+IBM-BMT+OT group. These results indicated that bone mass was maintained and increased after allogeneic OT, and that total body irradiation as a conditioning regimen for transplantation has toxic effects on the bone (Table 1).

Levels of Serum Estradiol and Urine DPD

There were no statistical differences between the sham-operated group and the OvX+IBM-BMT+OT group in the serum estrogen levels, suggesting that allogeneic ovaries transplanted under the kidney capsules were accepted and could secrete estrogen, resulting in maintaining normal estrogen levels in the OvX mice. The estrogen levels in the OvX+IBM-BMT group were the lowest in the three experimental groups; the OvX group was similar to the OvX+IBM-BMT group, while there was a significant difference between the OvX group and the OvX+ IBM-BMT+OT group. The levels of DPD released from the breakdown of collagen were measured in the urine to estimate osteoclast activity. The DPD levels in the OvX+IBM-BMT+OT group decreased, indicating that bone resorption decreased and bone turnover rate by OvX was suppressed after allogeniec OT. In the OvX+IBM-BMT group, however, the DPD levels were high, indicating that bone loss could not be prevented without OT (Table 2).

DISCUSSION

More and more cancer patients will be long-term survivors of radiochemotherapy and BMT, but a long lifespan does not necessarily imply a normal life. Especially in young women, ovarian failure and premature menopause have a strong impact on self-esteem and quality of life (*14–17*). Therefore, the lasting adverse effects of these modalities are receiving increasing attention.

Research during the last decade has revealed that estrogen regulates bone homeostasis through direct effects on bone cells. Estrogen deficiency results in an uncoupling of bone remodeling with a marked increase in bone resorption compared with bone formation.

Initiation of estrogen replacement therapy (ERT) in experimental animals and humans decreases erosion depth and

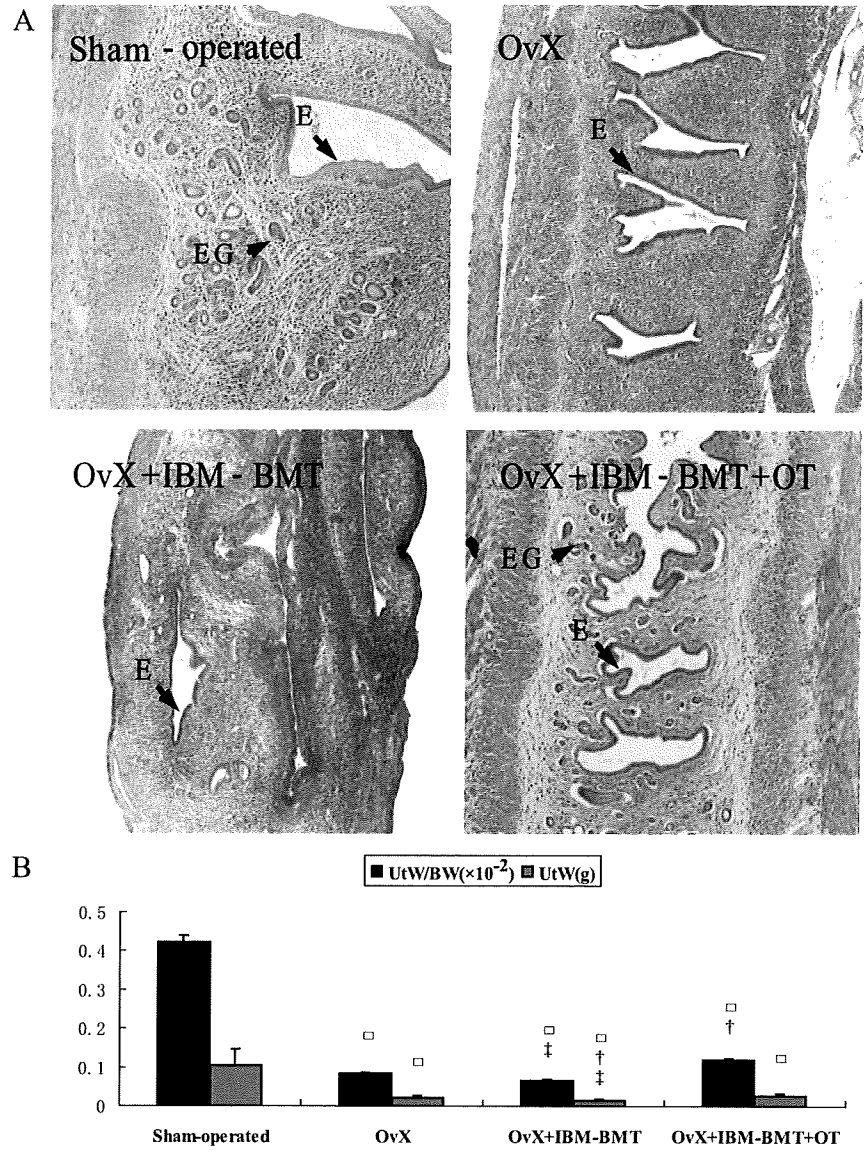

FIGURE 3. FEffects of IBM-BMT with OT on uterus. Three months after IBM-BMT, uteri of four groups (sham-operated group, OvX group, OvX+IBM-BMT group, and OvX+IBM-BMT+OT group) were sectioned and stained with hematoxylin and eosin. The OvX+IBM-BMT+OT group's uteri revealed normal endometrial glands (EG) and endometrium (E) morphology, but the other two experimental groups' uteri, especially the OvX+IBM-BMT group's uteri, revealed atrophic endometrium and few endometrial glands. Original magnification: ×100 for all panels (A). Uterus/body weight ratio and uterus weight were measured in the sham-operated group, OvX group, OvX+IBM-BMT+OT group, and OvX+IBM-BMT group. Data are expressed as mean ±SD, n=8. □$P<0.01$ vs. sham-operated group; †$P<0.01$ vs. OvX group; ‡$P<0.01$ vs. OvX+IBM-BMT+OT group (B).

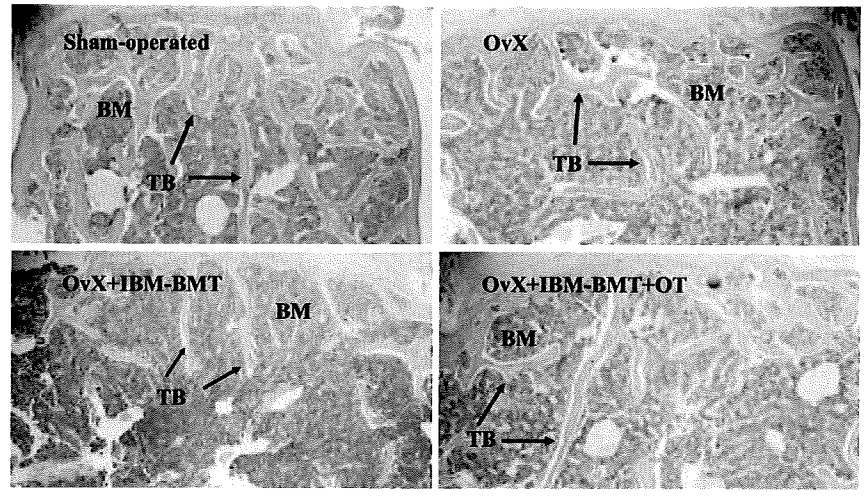

FIGURE 4. Histology of the lumbar vertebrae after IBM-BMT. Three months after IBM-BMT, the 4th lumbar vertebrae of mice in each of the four groups (sham-operated group, OvX group, OvX+IBM-BMT group, and OvX+IBM-BMT+OT group) were sectioned and stained with hematoxylin and eosin. Significant loss of trabecular bone (TB) was observed in the OvX group and the OvX+IBM-BMT groups; the trabeculars in the OvX+IBM-BMT group were short and small, but there were longer trabecular bones in the OvX+IBM-BMT+OT group. Original magnification: ×40 for all panels. BM, bone marrow.

TABLE 1. Effects of IBM-BMT with OT on L4 trabecular bone area and proximal tibia BMD in OvX mice

Group	L4 trabecular bone area percent (B.Ar/T.Ar)	Proximal tibia BMD (mg/cm^3)
Sham-operated	28.03±4.68	512.75±21.87
OvX	10.64±2.41[a]	445.58±27.61[a]
OvX+IBM-BMT	7.53±1.72 [a,b,c]	336.97±71.45[a,b,c]
OvX+IBM-BMT+OT	15.18±1.83[a,b]	442.10±29.34[a]

The OvX mice were treated for 3 months, and the L4 trabecular bone area and proximal tibia BMD were then measured by histomorphometry and pQCT, respectively. The trabecular bone area and proximal tibia BMD of the OvX+IBM-BMT+OT group increased, compared with the OvX+IBM-BMT group, indicating that bone formation increased. Data are expressed as means± SD, n=8.

[a] $P < 0.01$ vs. sham-operated group.

[b] $P < 0.01$ vs. OvX group.

[c] $P < 0.01$ vs. OvX+ IBM-BMT+OT group.

B.Ar/T.Ar, bone area/total area.

TABLE 2. Effects of IBM-BMT with OT on serum estrogen and urinary deoxypiridinoline (DPD) in OvX mice

Group	Serum estrogen (pg/mL)	Urinary DPD (nM)
Sham-operated	7.88±2.09	8.57±3.42
OvX	4.59±1.66[a]	14.01±6.28[a]
OvX+IBM-BMT	1.77±1.19[a,b,c]	18.95±6.16[a,b,c]
OvX+IBM-BMT+OT	7.69±1.71[b]	11.41±3.91[a]

Serum estrogen and urinary DPD were measured using ELISA kit. There were no significant differences between the sham-operated group and the OvX +IBM-BMT+OT group in serum estrogen assay. The hormonal rise indicated functioning allografts. In the DPD assay, the DPD level of the OvX+IBM-BMT+OT group declined compared with the OvX+IBM-BMT group, indicating that bone resorption decreased. Data are expressed as means± SD, n=8.

[a] $P < 0.01$ vs. sham-operated group.

[b] $P < 0.01$ vs. OvX group.

[c] $P < 0.01$ vs. OvX+IBM-BMT+OT group.

osteoclast activation frequency by stimulating apoptosis and blocking osteoclastogenesis (*18*). Estrogen therapy may decrease the rate of bone turnover by about 50% in the adult, resulting in fracture reduction at the spine, hip, and other sites of between 30% and 50% (*19*, *20*). However estrogen needs to be given for as long as the effect is required, within a few years of stopping hormone replacement therapy (HRT), the antifracture effect is no longer present (*21*).

The limitations in the use of estrogen are a consequence of the adverse effects. The Women's Health Initiative and The Million Women Study found an increased risk of stroke, coronary heart disease, and breast cancer associated with long-term treatment with HRT (*19*). Young women with premature ovarian failure need estrogen therapy for longer than older women, with the result that the adverse effects of exogenous estrogen will be more severe.

In this study, we carried out allogeneic IBM-BMT+OT on OvX mice to investigate the effects of endogenous estrogen secreted by allogeneic ovary, since we have recently proven in many animal experiments that different kinds of donor cells including HSCs could be efficiently recruited into the bone marrow by IBM-BMT, which leads to the rapid hemopoietic and immune recovery of recipients, inducing donor-specific tolerance in allogeneic organ transplantation, and promoting the survival rate of recipients (*8*, *9*).

In the present study, three months after the transplantation, the hematolymphoid cells were found to be completely reconstituted with donor-derived cells. The transplanted ovary tissues under the renal capsules were accepted without using immunosuppressants; even after 10 months, mature follicles were found in the allogeneic ovary engrafted after IBM-BMT without using any immunosupressants. The levels of endogenous estrogen were no different between the OvX+IBM-BMT+OT group and normal control group (sham-operated group). We know that irradiation can result not only in ovarian failure, but also in uterine dysfunction. However, in the present study, after IBM-BMT+OT, the ratio of uterus/body weight and uteri weight increased in the OvX+IBM-BMT+OT group. Moreover, endometrial morphology including endometrial glands was almost normal, although the uterine volume was still below the normal range. In another experiment, female mice without OvX received allogeneic IBM-BMT and allogeneic OT under the renal capsule after lethal irradiation. After 3 months, many immature follicles remained in the recipients' ovaries. It is well known that gonads are radiosensitive; low-dose irradiation can completely sterilize female mice. The immature follicles that remained in the recipients' ovaries had probably developed from germline stem cells (GSCs) residing in the recipients' ovaries (*22*) or from bone marrow (*23*) after IBM-BMT+OT. Also, after allogeneic IBM-BMT+OT as described above, in one group of mice we used the Johnson protocol (*22*) to transplant the allogeneic ovaries into the recipient's bursal cavity in contact with the remaining host ovarian. These mice were then mated with male mice. Two of 8 mice achieved pregnancy (data not shown). We therefore believe that IBM-BMT + OT may help promote the reconstitution of uterine functions.

The dominant acute effect of estrogen is the blockade of new osteoclasts formation. Osteoclasts arise by cytokine-driven proliferation and differentiation of monocyte precursors that circulate within the hematopoietic cell pool (*24*). This process is facilitated by bone marrow stem cells, which provide physical support for nascent osteoclasts and produce soluble and membrane-associated factors essential for the proliferation and differentiation of osteoclast precursors.

IBM-BMT can facilitate the early engraftment of hematopoietic cells of donor origin (*8*, *9*), indicating that it can generate normal osteoclasts in the bone marrow. As has been recently reported, BMCs contain not only HSCs (including osteoclast precursors), but also MSCs (including osteoblasts) (*25*). BM stromal cells can differentiate into osteoblasts, chondrocytes, adipocytes, cardiomyocytes, and even neurons (*26–28*). By IBM-BMT, not only donor-derived HSCs but also donor-derived MSCs can be recruited into the bone marrow site and can proliferate and differentiate. Estrogen can directly modulate the differentiation of bone marrow stromal cells into osteoblasts and increase the deposition and mineralization of matrix (*29*, *30*).

In the present study, mice were first ovariectomized to precipitate a marked reduction in endogenous estrogen con-

centrations and to induce bone remodeling abnormalities that augment bone loss and increase the risk of developing osteopenia or osteoporosis. We found that the bone mass in the OvX+IBM-BMT+OT group showed a significant increase after 3 months, while DPD as a biochemical bone resorption marker decreased compared with the OvX+IBM-BMT group, although the BMD did not regain the normal levels, in contrast to the sham-operated group. In another experiment, we noted that the bone mineral density of the OvX+IBM-BMT+OT group did not increase even after 6 months, compared with 3 months in the present experiment (data not shown). Lee youngwon et al. showed that the differentiation of bone marrow stromal cells into osteoblasts was impaired after BMT (*31*). On the other hand, Wang et al. reported that MSC transplantation can help to strengthen osteoporotic bone (*32*) without using irradiation as the conditioning regimen. Thus, the toxic effect of total body irradiation (TBI) on the bone is so severe and complicated (*33*, *34*) that we think both antiosteoporotic effects of endogenous estrogen secreted by the transplanted ovary and donor-derived MSCs were insufficient to establish normal BMD in 3 months; nonmyeloablative conditioning regimens may be substituted for TBI in future. We suggest that antiosteoporotic drugs are used as soon as possible after ovarian failure, and before and after BMT in clinical practice to prevent bone loss.

Many antiosteoporotic drugs are used to prevent and treat postmenopausal osteoporosis, but they do not have curative effects on symptoms such as hot flashes and the urogenital complaints induced by endogenous estrogen deficiency besides HRT (*35*, *36*).

From our results, we believe that IBM-BMT plus ovarian allografts would be advantageous for young women with primary or secondary estrogen deficiency (due to chemotherapy and radiation therapy in malignant diseases). Transplantation surgery is limited by the supply of fresh donor organs. It has been reported that cryopreserved intact ovary grafts succeeded in syngeneic rats (*37*). We believe that, if this new strategy can be shown to be safe for application to humans, IBM-BMT+OT could not only be used to treat cancer and prevent bone loss, but could also help promote the patient's self-esteem and quality of life.

ACKNOWLEDGMENTS

We thank Ms. Y. Tokuyama, K. Hayashi and A. Kitajima for their expert technical assistance. We also thank Mr. Hilary Eastwick-Field and Ms. K. Ando for their help in the preparation of the manuscript.

REFERENCES

1. Larsen EC, Loft A, Holm K, et al. Oocyte donation in women cured of cancer with bone marrow transplantation including total body irradiation in adolescence. *Hum Reprod* 2000; 15: 1505.
2. Schimmer AD, Quatermain M, Imrie K, et al. Ovarian function after autologous bone marrow transplantation. *J Clin Oncol* 1998; 16: 2359.
3. Salooja N, Szydlo RM, Socie G, et al. Pregnancy outcomes after peripheral blood or bone marrow transplantation: A retrospective survey. *Lancet* 2001; 358: 271.
4. Alper MM, Garner PR. Premature ovarian failure: Its relationship to autoimmune disease. *Obstet Gynecol* 1985; 66: 27.
5. Davis SR. Premature ovarian failure. *Maturitas* 1996; 23: 1.
6. Haukvik UKH, Dieset I, Bjøro T, et al. Treatment-related premature ovarian failure as a long-term complication after Hodgkin's lymphoma. *Ann Oncol* 2006; 17: 1428.
7. Notelovitz M. Clinical opinion: The biologic and pharmacologic principles of estrogen therapy for symptomatic menopause. *Med Gen Med* 2006; 288: 85.
8. Ikehara S. Intra-bone marrow-bone marrow transplantation: A new strategy for treatment of stem cell disorders. *Ann N Y Acad Sci* 2005; 1051: 626.
9. Kushida T, Inaba M, Hisha H, et al. Intra-bone marrow injection of allogeneic bone marrow cells: A powerful new strategy for treatment of intractable autoimmune diseases in MRL/lpr mice. *Blood* 2001; 97: 3292.
10. Jin T, Toki J, Inaba M, et al. A novel strategy for organ allografts using sublethal (7 Gy) irradiation followed by injection of donor bone marrow cells via portal vein. *Transplantation* 2001; 71: 1725.
11. Taira M, Inaba M, Takada K, et al. Treatment of streptozotocin-induced diabetes mellitus in rats by transplantation of islet cells from two major histocompatibility complex disparate rats in combination with intra bone marrow injection of allogeneic bone marrow cells. *Transplantation* 2005; 79: 680.
12. Esumi T, Inaba M, Ichioka N, et al. Successful allogeneic leg transplantation in rats in conjunction with intra-bone marrow injection of donor bone marrow cells. *Transplantation* 2003; 76: 1543.
13. Waterhouse T, Cox SL, Snow M, et al. Offspring produced from heterotopic ovarian allografts in male and female recipient mice. *Reproduction* 2004; 127: 689.
14. Schover L. Sexuality and body image in younger women treated for breast cancer. *J Natl Cancer Inst Monog* 1997; 16: 177.
15. Brenner PF. The menopausal syndrome. *Obstet Gynecol* 1988; 72: 68.
16. Ganz PA, Greendale GA, Petersen L, et al. Breast cancer in younger women: reproductive and late health effects of treatment. *J Clin Oncol* 2003; 21: 4184.
17. Ganz PA, Rowland JH, Desmond K, et al. Life after breast cancer: understanding women's health-related quality of life and sexual functioning. *J Clin Oncol* 1998; 16: 501.
18. Eriksen EF, Langdahl B, Vesterby A, et al. Hormone replacement therapy prevents osteoclastic hyperactivity: A histomorphometric study in early postmenopausal women. *J Bone Miner Res* 1999; 14: 1217.
19. Rossouw JE, Anderson GL, Prentice RL, et al. Risks and benefits of estrogen plus progestin in healthy postmenopausal women: Principal results from the Women's Health Initiative randomized controlled trial. *JAMA* 2002; 288: 321.
20. Torgerson DJ, Bell-Syer SE. Hormone replacement therapy and prevention of nonvertebral fractures: A meta-analysis of randomized trials. *JAMA* 2001; 285: 2891.
21. Michaelsson K, Baron JA, Farahmand BY, et al. Hormone replacement therapy and risk of hip fracture: Population based case control study. The Swedish Hip Fracture Study Group. *BMJ* 1998; 316: 1858.
22. Johnson J, Canning J, Kaneko T, et al. Germline stem cells and follicular renewal in the postnatal mammalian ovary. *Nature* 2004; 428: 145.
23. Johnson J, Bagley J, Skaznik-Wikiel M, et al. Oocyte generation in adult mammalian ovaries by putative germ cells in bone marrow and peripheral blood. *Cell* 2005; 122: 303.
24. Teitelbaum, S.L. Bone resorption by osteoclasts. *Science* 2000; 289: 1504.
25. Kushida T, Inaba M, Hisha H, et al. Crucial role of donorderived stromal cells in successful treatment for intractable autoimmune diseases in MRL/lpr mice by BMT via portal vein. *Stem Cells* 2001; 19: 226.
26. Pereira RF, O'Hara MD, Laptev AV, et al. Marrow stromal cells as a source of progenitor cells for nonhematopoietic tissues in transgenic mice with a phenotype of osteogenesis imperfecta. *Proc Natl Acad Sci USA* 1998; 95: 1142.
27. Makino S, Fukuda K, Miyoshi S, et al. Cardiomyocytes can be generated from marrow stromal cells in vitro. *J Clin Invest* 1999; 103: 697.
28. Woodbury D, Schwarz EJ, Prockop DJ, Black IB. Adult rat and human bone marrow stromal cells differentiate into neurons. *J Neurosci Res* 2000; 61: 364.
29. Okazaki R, Inoue D, Shibata M, et al. Estrogen promotes early osteoblast differentiation and inhibits adipocyte differentiation in mouse bone marrow stromal cell lines that express estrogen receptor (ER)$-\alpha$ or $-\beta$. *Endocrinology* 2002; 143: 2349.
30. Qu Q, Perala-Heape M, Kapanen A, et al. Estrogen enhances differentiation of osteoblasts in mouse bone marrow culture. *Bone* 1998; 22: 201.

31. Lee WY, Cho SW, Oh ES, et al. The effect of bone marrow transplantation on the osteoblastic differentiation of human bone marrow stromal cells. *J Clin Endocrinol Metab* 2002; 87: 329.
32. Wang Z, Goh J, Das De S. Efficacy of bone marrow-derived stem cells in strengthening osteoporotic bone in a rabbit model. *Tissue Eng* 2006; 12: 1753.
33. Ergun H, Howland WJ. Postradiation atrophy of mature bone. *CRC Crit Rev Diagn Imaging* 1980; 12: 225.
34. Hopewell JW. Radiation-therapy effects on bone density. *Med Pediatr Oncol* 2003; 41: 208.
35. Keller PJ, Maurer-Major E. Hormone substitution in menopause. *Schweiz Rundsch Med Prax* 1997; 86: 1458.
36. Ness J, Aronow WS, Beck G. Menopausal symptoms after cessation of hormone replacement therapy. *Maturitas* 2006; 53: 356.
37. Wang X, Chen H, Yin H, et al. Fertility after intact ovary transplantation. *Nature* 2002; 415: 385.

Clinical and Experimental Immunology ORIGINAL ARTICLE doi:10.1111/j.1365-2249.2008.03588.x

The Wistar Bonn Kobori rat, a unique animal model for autoimmune pancreatitis with extrapancreatic exocrinopathy

Y. Sakaguchi,*† M. Inaba,* M. Tsuda,* G. K. Quan,* M. Omae,* Y. Ando,* K. Uchida,† K. Okazaki† and S. Ikehara*

**First Department of Pathology and †Third Department of Internal Medicine, Kansai Medical University, Moriguchi City, Osaka, Japan*

Accepted for publication 4 December 2007
Correspondence: S. Ikehara, First Department of Pathology, Kansai Medical University, 10-15 Fumizono-cho, Moriguchi City, Osaka 570-8506, Japan.
E-mail: ikehara@takii.kmu.ac.jp

Summary

The male Wistar Bonn/Kobori (WBN/Kob) rat is known to be a unique animal model for chronic pancreatitis with widely distributed fibrosis and degeneration of parenchyma because of the infiltration of lymphocytes. In this report, we show that female (but not male) rats develop dacryoadenitis at 3 months of age, and that both male and female WBN/Kob rats develop sialoadenitis, thyroiditis, sclerotic cholangitis and tubulointerstitial nephritis over 18 months of age. The infiltration of $CD8^+$ cells and the deposits of tissue-specific IgG2b were observed in the injured pancreas and lachrymal glands. Furthermore, the number of regulatory T cells (defined as $CD4^+$ Forkhead box $P3^+$ cells) decreased in the periphery of both male and female WBN/Kob rats, suggesting that the onset of these diseases is attributable, at least, to the failure in the maintenance of peripheral immune tolerance. These features show clearly that WBN/Kob rats are a useful animal model for autoimmune pancreatitis and Sjøgren-like syndrome or multi-focal fibrosclerosis in humans. We also show that these autoimmune diseases can be prevented by a newly devised strategy of bone marrow transplantation (BMT) in which bone marrow cells are injected directly into the bone marrow cavity: intrabone marrow–BMT.

Keywords: animal model, autoimmune extrapancreatic exocrinopathy, autoimmune pancreatitis, Forkhead box P3, intra bone marrow–bone marrow transplantation

Introduction

Recently, autoimmune pancreatitis (AIP) has been reported as a part of chronic pancreatitis with pancreatic duct stenosis. AIP is characterized by hypergammaglobulinaemia and responsiveness to corticosteroid therapy, suggesting the involvement of autoimmune mechanisms, particularly at the onset of this disease [1]. Patients with autoimmune diseases such as Sjøgren's syndrome and other autoimmune diseases in the liver, bile ducts, intestine and blood vessels often show AIP [2]. Lesions in the pancreas have been observed in acinar cells, ductal cells and pancreatic islet cells, indicating that the target cells or target molecules for autoimmune reactions are considered to be variable [3]. The precise mechanism underlying the onset of AIP and its progress is still unknown [4], although the diagnosis and therapy have been investigated extensively and progressed. In various cases of pancreatitis, it is difficult to prove whether autoimmune mechanisms are involved in the development of pancreatitis [5]. Therefore, long-term studies on histopathological evaluation before the onset of pancreatitis are clinically important [6]. Imaging studies of patients with AIP characteristically show the diffuse enlargement of the pancreas and irregular narrowing of the main pancreatic duct. Typical immunological abnormalities are the elevation of serum IgG4 and the presence of autoantibodies. The histopathological findings show lymphoplasmacytic sclerosing pancreatitis (LPSP) associated with fibrotic changes with dense infiltration of lymphocytes and IgG4-positive plasma cells [7]. However, the role of IgG4 in the pathogenesis of AIP still remains unclear. Therefore, the establishment of an animal model for AIP is critically important. To date, there have been reported various artificial AIP models, most of which are chemical or antigen-induced ones [8,9]. Even if there are some spontaneous animal models which partially resemble human AIP [10,11], there are many differences in terms of symptoms, gene functions and pathological findings.

It has been shown that the male Wistar Bonn/Kobori (WBN/Kob) rat is an animal model for spontaneous diabetes, osteopenia and systemic haemosiderin deposition

[12]. Spontaneous hyperglycaemia, glycosuria, hypoinsulinaemia and glucose intolerance are observed after the age of 17 months. Marked fibrosis is observed around the pancreatic ducts and blood vessels at 3–6 months of age [13,14]. The fibrous tissue gradually invades extensive areas of the pancreas, and the islets are also affected by fibrotic degeneration, leading to an obvious decrease in islet number and size. Distinct infiltration of inflammatory cells has been observed around the islets and among adjacent acinar cells, and most inflammatory cells are apparently lymphocytes. Macrophages or granulocytes are not often observed in the lesions. These pathological findings are found in male but not female WBN/Kob rats, and have been discussed regarding their pathogenesis in relation to sex hormone [15], genetic factor [16] and immune disturbance [17]. WBN/Kob rats have some interesting characteristics: (i) only male WBN/Kob rats appear with pancreatitis; (ii) they are a unique diabetic animal model whose islets are withered by progress with inflammatory fibrosis dissimilar to the other diabetic models [18,19]; (iii) infiltrating cells are nearly all lymphocytes, rather than plasma cells and eosinophils [12]; and (iv) immune suppressive drugs such as tacrolimus or steroid hormones could prevent the onset of pancreatitis [17]. These characteristics resemble human AIP.

We have shown previously that conventional allogeneic bone marrow transplantation (BMT) can be used to treat autoimmune disease using various autoimmune-prone mice [20,21]. Recently, we have developed a new BMT method in which donor bone marrow cells (BMCs) are injected directly into the bone marrow cavity of recipients: intrabone marrow–BMT (IBM–BMT) [22,23]. This strategy allows us to reduce radiation doses to 5 Gy × 2 (fractionated irradiation), which is equivalent to 8 Gy (one shot). Therefore, we attempted to prevent abnormal pathological, serological and immunological findings in the WBN/Kob rats by IBM–BMT; in our preliminary experiments, conventional BMT was found to be unable to be used to prevent these abnormalities in the rats. In line with these studies, the model described here can be considered to be highly relevant not only for a better understanding of the pathogenesis of AIP but also for the preclinical testing of novel strategies for the treatment of AIP.

Materials and methods

Rats

Male and female WBN/Kob rats (RT1a^u), male Wistar rats and Fischer 344 (F344:RT1a^l) rats were purchased from SLC (Shizuoka, Japan). They were maintained until use in our animal facilities under specific pathogen-free conditions. All experimental protocols were approved by the Animal Experimentation Committee (06-026), Kansai Medical University.

Histopathological analysis

Histopathological studies of the systemic exocrine organs (pancreas, liver, lachrymal and parotid glands, kidney and thyroid) in male and female WBN/Kob rats 4 weeks, 12 weeks and 18 months of age were performed. In brief, each organ was fixed in paraformaldehyde and infiltrated with Histo-Clear (National Diagnostics, Atlanta, GA, USA) [24]. They were dehydrated with ethanol and embedded in paraffin (5 μm), and stained with haematoxylin and eosin or Masson-Trichrome and Sirius red to detect fibrosis.

Immunohistochemical analyses

Thyroid, liver and kidney from 18-month-old WBN/Kob rats, and pancreas, spleen, lachrymal gland and parotid gland were obtained serially from the recipients 4, 8, 12 and 16 weeks after IBM–BMT. The sections were prepared with the masked antigen for using Histo-Clear, rehydrated through a graded series of ethanol/water solutions and incubated at 85°C in antigen retrieval buffer. The specimens were also stained with fluorescein isothiocyanate (FITC)-, phycoerythrin (PE)- or biotin-conjugated IgG, IgG1, IgG2a, IgG2b and IgG2c (FITC–streptavidin was used to visualize biotin-conjugated antibodies). Nuclei were stained with 4,6-diamidino-2-phenylindole (Nacalai Tesque, Inc., Kyoto, Japan). Immunohistochemical staining for CD4$^+$, CD8$^+$ cells, anti-major histocompatibility complex (MHC) I (OX-18) and anti-MHC II (OX-6) were also performed using frozen tissues from pancreas and lachrymal gland. The sections (4 μm) were incubated with appropriate primary antibodies at 4°C overnight. They were incubated with biotinylated secondary anti-rat IgG antibodies (Vector Laboratories, Burlingame, CA, USA) and incubated with avidin–biotin horseradish peroxidase complex (Vector Laboratories). Samples were incubated with 3,3′-diaminobenzidine in the presence of H_2O_2 to develop the chromatic reaction. The stained samples were analysed using an optical microscope (Nikon Eclipse E1000M, Digital Sight ACT-1 for L-1 software version 2·62; Nikon Co. Ltd, Tokyo, Japan) and confocal laser microscope (LSM 510 META; Carl Zeiss IMT Corporation, Oberkochen, Germany).

Biochemical analyses

Blood glucose was measured by a Dextor ZIIR (Bayer Medical Ltd, Tokyo, Japan). Total amylase and total protein were determined by a biochemistry automated analyser (AU5400; Olympus Corp., Tokyo, Japan). Immunoelectrophoresis was carried out in our laboratory using standard equipment. Interleukin (IL)-4, IL-10 and IL-12 were analysed by an enzyme-linked immunosorbent assay kit (R&D Systems, Inc., Minneapolis, MN, USA; BioSource, Camarillo, CA, USA).

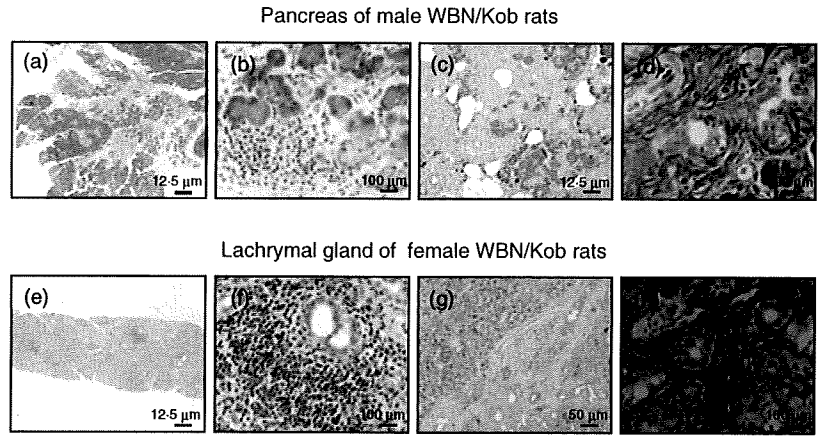

Fig. 1. Pathological findings of pancreas and lachrymal grand of male and female Wistar Bonn/Kobori (WBN/Kob) rats. Paraffin sections of pancreas and lachrymal gland were prepared and stained with haematoxylin and eosin (H&E) (6 months of age). (a,b,e,f) Stained with H&E, (c) and (g); stained with Masson-Trichrome, (d) and (h); stained with Sirius red. Bars in the figure represent scales.

IBM–BMT experiments

Fludarabine at 50 mg/kg was given as a single intravenous injection and irradiated in fractionated irradiations (5·0 Gy × 2 = 10 Gy; 4-h interval) 1 day before transplantation. BMCs were collected from the femurs and tibias of Fischer 344 rats. $CD4^+$ cells were depleted from the BMCs by the combination of anti-CD4 antibody (Caltag Laboratories, Burlingame, CA, USA) and sheep anti-mouse IgG-coupled Dynabeads® (Dynal, Oslo, Norway). Resultant $CD4^+$ T cell-depleted BMCs (2×10^8 BMCs) were injected directly into the bone marrow cavity of the recipient's tibia (IBM–BMT) to facilitate the early recovery of haematopoiesis and donor cell engraftment [22]. In brief, the region from the thigh to the knee joint was shaved of hair with a razor. The knee was flexed to 90°, and the proximal side of the tibia was drawn to the anterior. A 21-gauge needle was inserted into the joint surface of the tibia through the patellar tendon and then inserted into the bone marrow cavity. Using a microsyringe (50 μl; Hamilton Co., Reno, NV, USA), the donor BMCs (3×10^7/30 μl) were injected into the bone marrow cavity. These WBN/Kob rats are abbreviated as (F344→WBN/Kob).

Surface marker analyses

The spleen cells, peripheral blood mononuclear cells or BMCs were prepared from recipient rats, and the cells were then stained with FITC-anti-$RT1A^l$ monoclonal antibodies (mAb) (PharMingen, San Diego, CA, USA) to identify the donor-derived cells. Donor-derived cells bearing a lineage-specific phenotype were also analysed by FITC-anti-$RT1A^l$ mAb plus PE-conjugated mAb against CD45R (B220) (PharMingen), CD4, CD8 or CD11b (Caltag Laboratories). Furthermore, the cells were stained with anti-CD4 and anti-CD25 mAb (BD Pharmingen, Hamburg, Germany) or anti-CD4 and anti-Forkhead box P3 (FoxP3) mAb to detect regulatory T cells (T_{regs}). In the case of staining with anti-FoxP3 mAb, cells were stained with FITC-anti-CD4 mAb, and then fixed and permeabilized with Cutofix/Cytoperm solution™ (BD Pharmingen). The cells thus treated were stained intracytoplasmically with PE-anti-FoxP3 mAb (eBioscience, Inc., San Diego, CA, USA). The stained cells were analysed by a fluorescence activated cell sorter (FACScan®; Becton Dickinson, Mountain View, CA, USA).

Statistical analysis

Survival data were analysed using the Kaplan–Meier method using StatMate software. Differences between groups were analysed using the log-rank test in the StatMate software. $P < 0.05$ was considered to be significant.

Results

Histopathological and immunological features of WBN/Kob rats

After 4 weeks of age male WBN/Kob rats showed chronic pancreatitis, while after 4 weeks of age female WBN/Kob rats showed Sjøgren-like dacryoadenitis. Histopathologically, significant oedema in the interstitium, the infiltration of lymphocytes and the destruction of acinar cells were seen in the pancreas of male WBN/Kob rats (Fig. 1a and b). At approximately 8 weeks of age fibrosis appeared in the lobules, and after 12 weeks of age the infiltration of inflammatory cells, oedema, haemorrhage and the deposit of haemosiderin were found in the interlobules or peri-pancreatic ducts, leading to the isolation of acini and pancreatic islets, followed by acceleration of fibrosis (Fig. 1c and d). On the other hand, in female WBN/Kob rats, the infiltration of inflammatory cells was found in the outer lachrymal glands after the age of 4 weeks, and the inflammation was aggravated dually. Significant infiltration of lymphocytes was noted in the periductal area, and the acceleration of fibrosis was found in the interlobules (Fig. 1g and h), although the lobular structure in the outer lachrymal glands was still maintained (Fig. 1e and f). Furthermore, many vacuoles and the degeneration

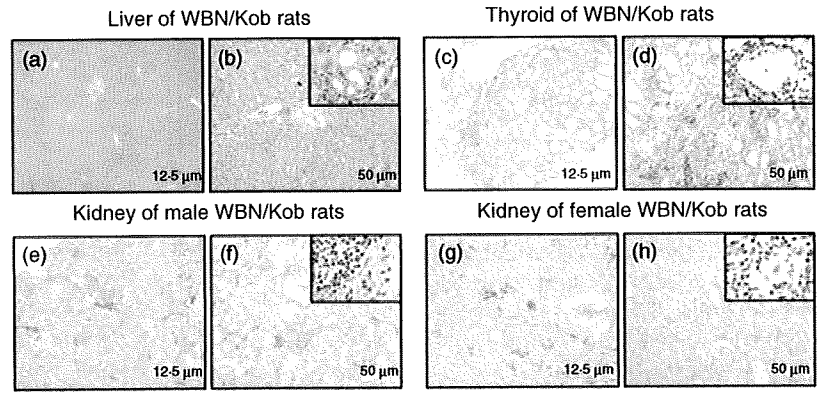

Fig. 2. Pathological findings of liver, thyroid and kidney in the aged Wistar Bonn/Kobori (WBN/Kob) rats. Twenty months after birth, liver, thyroid and kidney were removed and paraffin sections were stained with haematoxylin and eosin. (a, b) Liver; (c,d) thyroid; (e,f) kidney of male WBN/Kob rat; (g,h) kidney of female WBN/Kob rat.

of nucleus structure were detected in acinar cells. Thus, chronic dacryoadenitis (and partially parotiditis) resembling Sjøgren's syndrome was found in female WBN/Kob rats.

In aged male and female WBN/Kob rats (>18 months of age), sclerotic cholangitis, thyroiditis and even tubulointerstitial nephritis were observed along with pancreatitis and dacryoadenitis. The infiltration of inflammatory cells was found in the area of peripheral bile ducts, and hyperplasia of bile ducts and the fibrosis of peri-bile duct areas were also observed (Fig. 2a and b), resembling sclerotic cholangitis in humans. Colloids in the thyroid glands were found to be degenerated and partially destroyed. Infiltration of the inflammatory cells was detected in hyperplastic and fibrous interstitium (Fig. 2c and d). Furthermore, in male WBN/Kob rats, the hyperplasia of the mesangial cells and the demilune bodies in the uriniferous tubule were found clearly as evidence of diabetic nephritis associated with tubulointerstitial nephritis. Infiltration of the inflammatory cells was also detected in the interstitium as tubulointerstitial nephritis (Fig. 2e and f). On the other hand, infiltration of the inflammatory cells was detected only in the interstitium in female WBN/Kob rats where pancreatitis was not developed (Fig. 2g and h). Thus, it is noted that there are clear sex differences in pathological findings.

Immunohistochemical analyses revealed that a large number of $CD8^+$ T cells were observed in the injured organs (Fig. 3b pancreas; Fig. 3f lachrymal gland), while a small number of $CD4^+$ T cells were infiltrated into the pancreas (Fig. 3a) and lachrymal gland (Fig. 3e). The expression of both MHC class II (Fig. 3c pancreas; Fig. 3g lachrymal gland) and MHC class I (Fig. 3d pancreas; Fig. 3h lachrymal gland) was also found, although the former was less than the latter.

Serum γ-globulin levels increased in both male and female WBN/Kob rats (Fig. 4), and the deposits of γ-globulin were also observed in the pancreas of male WBN/Kob rats and in the lachrymal gland of female rats. IgG, which was detected specifically in the injured region, was IgG2b subclass, but not any other subclass (Fig. 5) (IgG2c appeared with non-specific staining), and IgG2b was actually detected in the B cells which appeared in the injured region (Fig. 6i and j pancreas; Fig. 6l and m lachrymal gland) along with $CD8^+$ T cells (Fig. 6c pancreas; Fig. 6h lachrymal gland). These findings indicate clearly that pancreatitis in male WBN/Kob rats and dacryoadenitis in female WBN/Kob rats develop as a result of immunological disorders, and can be categorized as AIP and autoimmune dacryoadenitis.

The involvement of immunological disorders in the onset of pancreatitis and dacryoadenitis was confirmed by the measurement of T_{regs} known to control negatively autoreactive T cells in the periphery. When compared with normal controls (F344), the number of T_{regs} (detected as $CD4^+$ $FoxP3^+$ cells in the spleen cells) was decreased significantly in WBN/Kob rats (~7% in WBN/Kob rats at 8 weeks, ~10% in

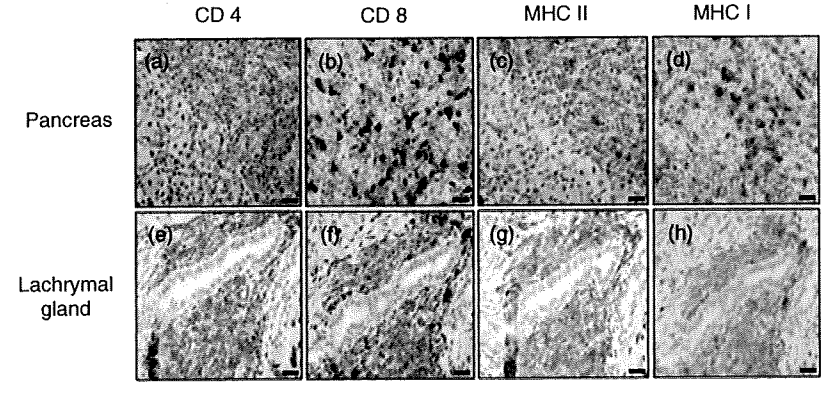

Fig. 3. Immunohistological staining for $CD4^+$, $CD8^+$, major histocompatibility complex (MHC) I and anti-MHC II T cells. Pancreas and lachrymal gland were removed (4 months of age) and serial sections were stained with anti-CD4, anti-CD8 anti-MHC I and anti-MHC II monoclonal antibody. (a–d) Pancreas of male Wistar Bonn/Kobori (WBN/Kob) rat; (e–h) pancreas of female WBN/Kob rat.

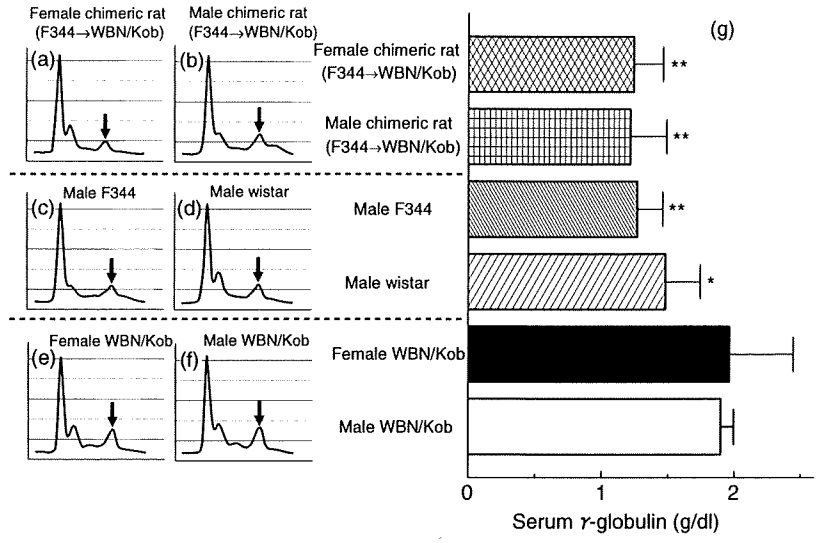

Fig. 4. Analyses of serum γ-globulin. Sera were collected from male and female Wistar Bonn/Kobori (WBN/Kob) rat (4 months of age) and electrophoresis was carried out to examine the relative level of IgG. (a) Female WBN/Kob rat treated with intrabone marrow–bone marrow transplantation (IBM–BMT) from F344 (F344→Kob); (b) male WBN/Kob rat treated with IBM–BMT from F344 (F344→WBN/Kob); (c) male F344 rat as a normal control; (d) male Wistar rat as a normal control; (e) untreated female WBN/Kob rat; (f) untreated male WBN/Kob rat; and (g) amounts of γ-globulin in sera calculated from the results of electrophoresis and total amounts of serum protein. Columns and bars represent means ± standard deviations of seven rats. $^*P < 0{\cdot}05$; $^{**}<0{\cdot}01$.

untreated normal F344 rats). The frequency of T_{regs} decreased gradually to ~4% in male WBN/Kob rats and to ~6% in females at 20 weeks (Fig. 7f), and the representative fluorescence activated cell sorter profiles are shown in Fig. 6a–e.

Effects of IBM–BMT on the development of pancreatitis and dacryoadenitis

We have found recently that IBM–BMT can facilitate the engraftment of not only donor-derived haemopoietic cells but also mesenchymal stem cells (bone marrow stromal cells), and thereby prevent or treat various intractable diseases [22,25,26]. We therefore applied this strategy to the prevention of pancreatitis and dacryoadenitis in WBN/Kob rats.

We first examined chimerism in the WBN/Kob rats that had received BMCs of donor F344 rats by IBM–BMT [(F344→WBN/Kob)]. Chimerism was analysed flow cytometrically using FITC-conjugated donor-specific anti-$RT1A^l$ mAb. As shown in Fig. 7 [compare (a, b, c) with (d,e)], haematolymphoid cells were of donor origin and the donor chimerism remained stable until the experiments were finished (20 weeks of age). The tolerant state was confirmed by mixed lymphocyte reaction. Splenic T cells from (F344→WBN/Kob) rats were used as responders and stimulated with irradiated spleen cells from F344 and unrelated BN rats. T cells from (F344→Kob) rats responded significantly to the unrelated BN spleen cells, but not to the spleen cells of F344 or WBN/Kob rats (data not shown), indicating that the T cells of (F344→WBN/Kob) rats were tolerant of the donor and recipient MHCs, but could respond to the third-party MHC determinants.

After IBM–BMT, the male or female recipients [(F344→WBN/Kob)] did not develop pancreatitis (Fig. 8b and c) or dacryoadenitis (Fig. 8g and h) respectively, showing no hyperglycaemia for more than 16 months (Fig. 9b) after IBM–BMT in the male recipients [(F344→WBN/Kob)], whereas chronic pancreatitis (Fig. 8d and e) or dacryoadenitis (Fig. 8i and j) was observed in the untreated WBN/Kob rats with the destruction of pancreatic islets, and hyperglycaemia was observed at 1 month and thereafter elevated gradually more than 400 mg/dl at 20 weeks of age. Infiltration of $CD8^+$ and $CD4^+$ T cells in the pancreas or lachrymal glands was not detected in the recipients [(F344→WBN/Kob)] (data not shown), and the frequency of T_{regs} in the periphery and spleen was normalized in both male and female (F344→WBN/Kob) rats and maintained even 20 weeks after IBM–BMT (Fig. 7f).

In accordance with the amelioration of pancreatitis or dacryoadenitis, serum amylase (Fig. 9a) and γ-globulin levels (Fig. 4) were normalized, and hyperglycaemia observed in the untreated male WBN/Kob rats was not detected (Fig. 9b).

Measurement of cytokines

To analyse the mechanism underlying the development of AIP and dacryoadenitis in the WBN/Kob rats, we next examined kinetically the cytokine levels of untreated WBN/Kob rats. The production of IL-10 in male and female WBN/Kob rats decreased at 3 months of age and remained unchanged to 20 months (Fig. 9f). In contrast, serum IL-12 levels in WBN/Kob rats increased at the age of 3 months, and the elevated levels of IL-12 were maintained until 20 months (Fig. 9d). The levels of IL-4 were slightly higher in male and female WBN/Kob rats than in the control male F344 rats, but there was statistically no significant difference between them (Fig. 9e).

Discussion

This study was carried out to clarify whether autoimmune mechanisms are involved in the development of pancreatitis

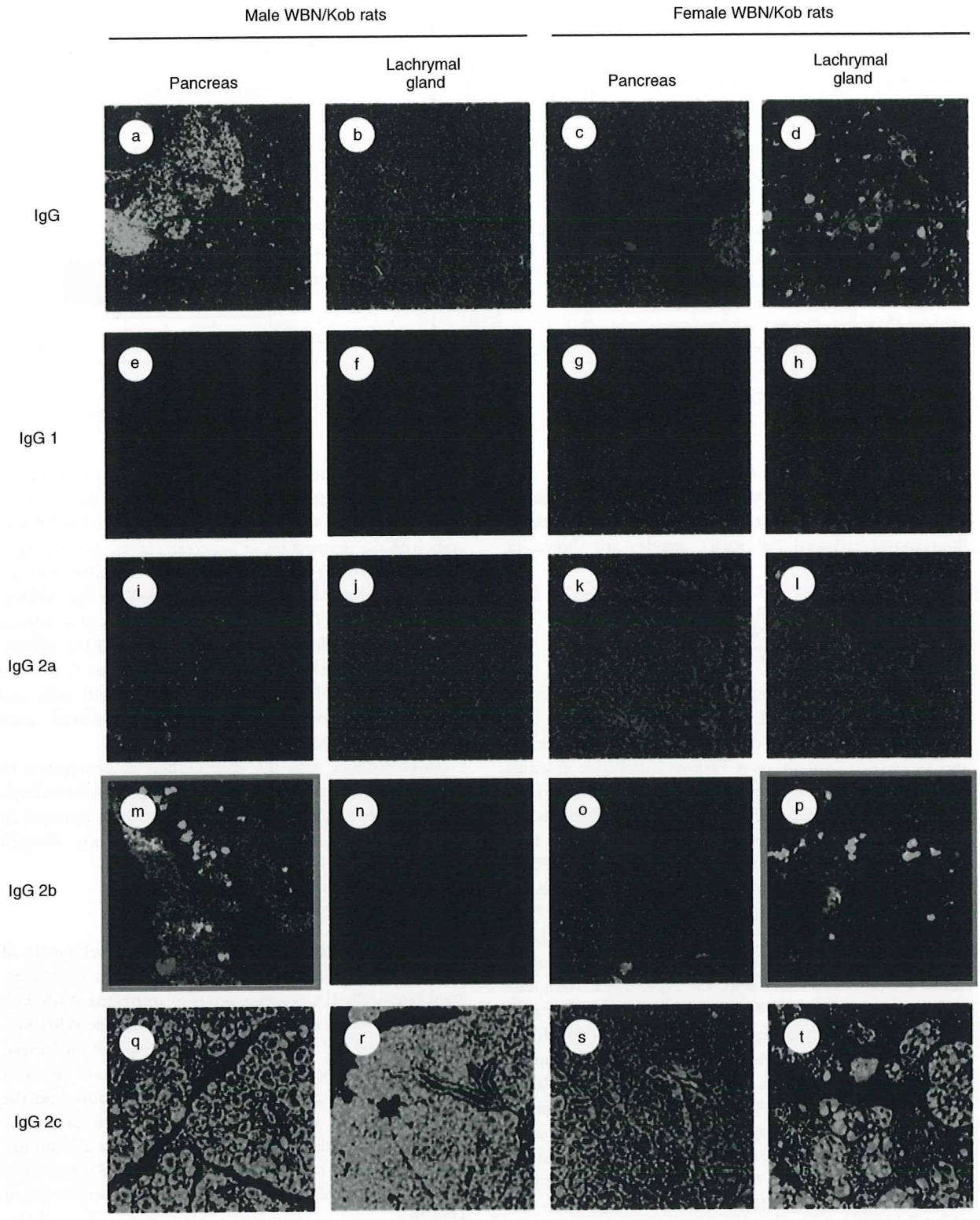

Fig. 5. Detection of tissue-specific antibody. Paraffin sections of pancreas and lachrymal gland were prepared from male and female Wistar Bonn/Kobori (WBN/Kob) rats (4 months of age) and stained with biotinylated anti-IgG (a–d), anti-IgG1 (e–h), anti-IgG2a (i–l), anti-IgG2b (m–p) or IgG2c (q–t). They were visualized by additional staining with fluorescein isothiocyanate–streptavidin.

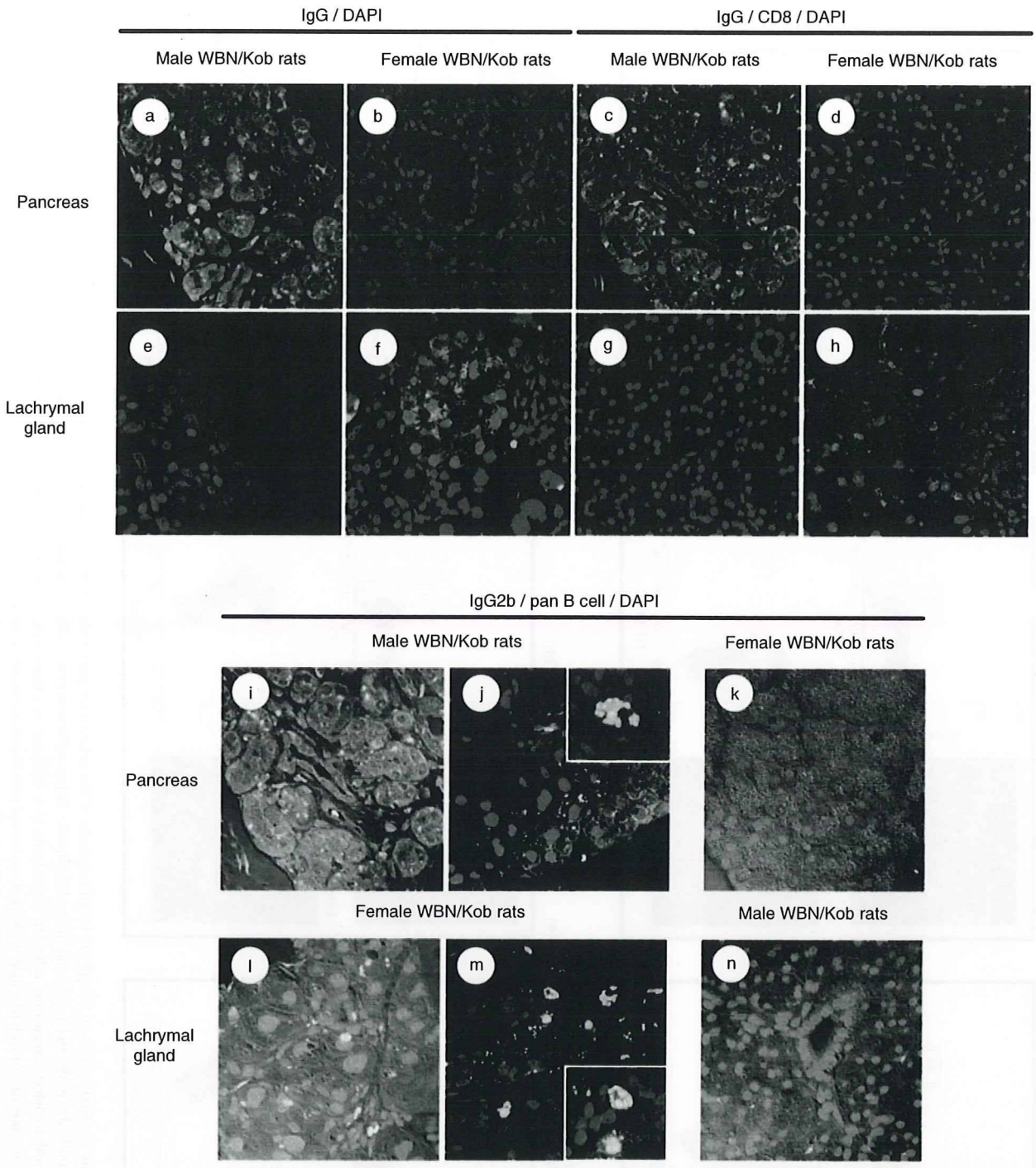

Fig. 6. Detection of infiltrated IgG-producing cells and $CD8^+$ T cells. Paraffin sections of pancreas and lachrymal gland were prepared from male and female Wistar Bonn/Kobori (WBN/Kob) rats (4 months of age) and stained with biotinylated anti-IgG monoclonal antibodies (mAb). (a,b) Pancreas; (e,f) lachrymal gland) followed by fluorescein isothiocyanate (FITC)–streptavidin. Nuclei were stained by 4,6-diamidino-2-phenylindole (DAPI). Paraffin sections were double-stained with anti-IgG mAb plus phycoerythrin (PE)-anti-CD8 mAb. (c,d) Pancreas; (g,h) lachrymal gland. Paraffin sections of the pancreas and lachrymal gland were stained with anti-IgG2b followed by FITC–streptavidin, PE-anti-pan B cell mAb and DAPI. (i–k) Pancreas; (l–n) lachrymal gland).

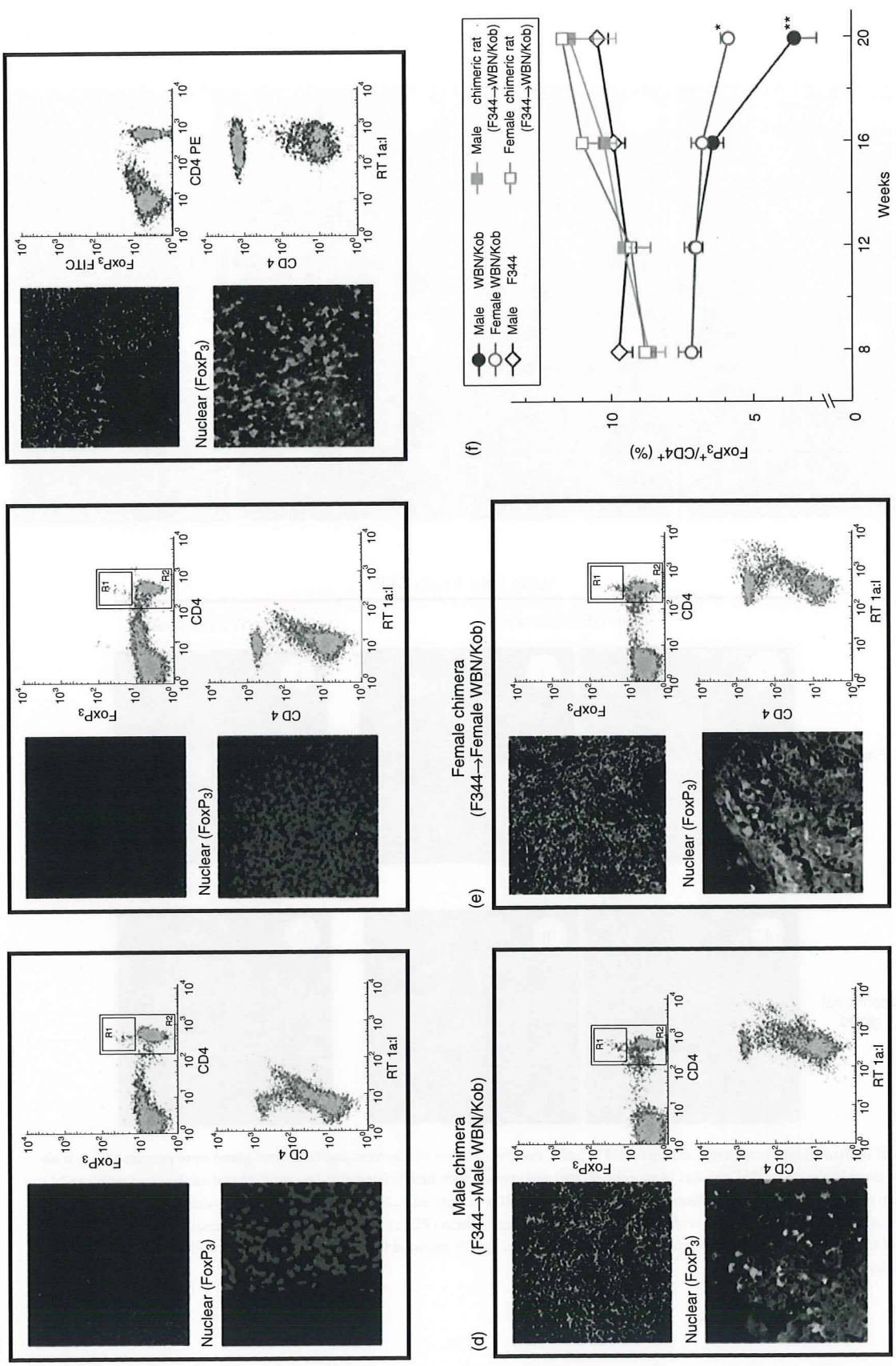

Fig. 7. Detection of Forkhead box P3 (FoxP3)$^+$ cells in the spleen. Paraffin sections of the spleen were prepared (4 months of age) and stained with fluorescein isothiocyanate (FITC)-anti-FoxP3 monoclonal antibody (mAb) and 4,6-diamidino-2-phenylindole. Spleen cells were prepared and stained with FITC-anti-CD4 mAb followed by the intracytoplasmic staining with phycoerythrin (PE)-anti-FoxP3 mAb to detect T regulatory cells. The stained cells were analysed by a fluorescence activated cell sorter scan. (a) Male Wistar Bonn/Kobori (WBN/Kob) rat; (b) female WBN/Kob rat; (c) male F344 rat as a normal control; (d) male WBN/Kob rat treated with intrabone marrow–bone marrow transplantation (IBM–BMT) from F344; (e) female WBN/Kob rat treated with IBM–BMT from F344). Spleen cells were also stained with FITC-anti-RT1A^1 [donor type rat major histocompatibility complex (MHC)] and PE-anti-CD4 mAbs to detect donor-derived cells. (a) Male WBN/Kob rat; (b) female WBN/Kob rat; (c) male F344 rat as a normal control; (d) male WBN/Kob rat treated with IBM–BMT from F344; (e) female WBN/Kob rat treated with IBM–BMT from F344). The frequency of FoxP3$^+$/CD4$^+$ cells was measured kinetically and summarized in Fig. 7F. Symbols and bars represent means ± standard deviations of seven rats. $^*P < 0{\cdot}05$.

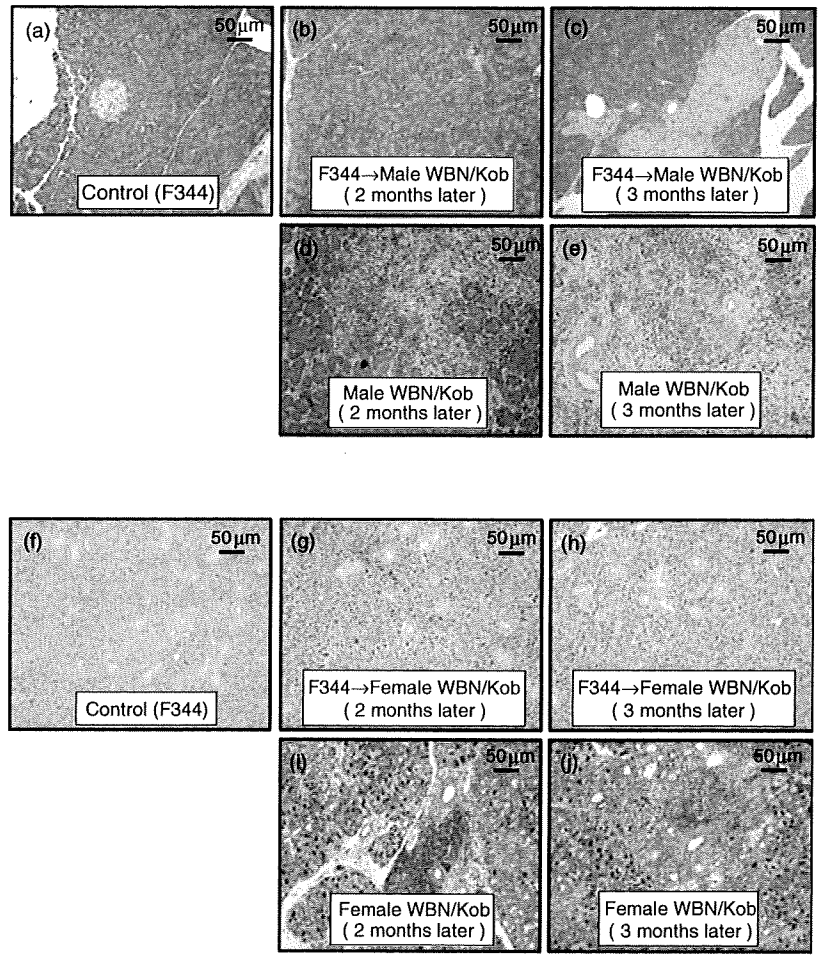

Fig. 8. Pathological findings of pancreas and lachrymal gland after intrabone marrow–bone marrow transplantation (IBM–BMT). Male and female Wistar Bonn/Kobori (WBN/Kob) rat treated with IBM–BMT from F344 (F344→WBN/Kob) were examined histologically after staining with haematoxylin and eosin. Paraffin sections of pancreas and lachrymal grand were prepared. (a–e) Pancreas; (f–j) lachrymal gland. (a) Male F344 rat as a normal control; (b) male WBN/Kob rat treated with IBM–BMT from F344 (F344→WBN/Kob, 3 months of age, 2 months after IBM–BMT); (c) male F344→WBN/Kob, 4 months of age, 3 months after IBM–BMT; (d) male WBN/Kob rat 3 months of age; (e) male WBN/Kob rat 4 months of age; (f) female F344 rat as a normal control; (g) female F344→WBN/Kob, 3 months of age, 2 months after IBM–BMT; (h) female F344→WBN/Kob, 4 months of age, 3 months after IBM–BMT; (i) female WBN/Kob rat 3 months of age; (j) female WBN/Kob rat 4 months of age.

in WBN/Kob rats, which allowed us to understand more clearly the pathogenic mechanism of AIP. Recently, AIP has been divided histologically into two distinctive types, LPSP and granulocyte epithelial lesion (GEL). In Japan and Korea, most patients with AIP show the LPSP type associated with systemic exocrinopathy in the aged male. By contrast, in Caucasians, younger patients with the GEL type of AIP associated with ulcerative colitis are often observed without gender difference as well as LPSP. The LPSP type of AIP has been thought to be a multi-focal fibrosclerosing disease with abundant infiltration of IgG4-positive plasmacytes, because extrapancreatic lesions, such as sclerosing cholangitis, sialoadenitis or dacryoadenitis (similar to Mikulicz's disease or Kuttner's tumour), retroperitoneal fibrosis, interstitial nephritis or thyroiditis, are often associated with AIP. It is noted that these lesions can be treated by administration of steroid hormone [27], suggesting that sclerosing cholangitis or sialoadenitis with AIP is different from primary sclerosing cholangitis or typical Sjøgren's syndrome respectively [28].

In the present study, we found that WBN/Kob rats showed different manifestations, depending on gender. In the pancreas of the male rats, many lymphocytes infiltrated around the pancreatic ducts, which seemed to destroy the pancreatic ducts and acinar cells. On the other hand, the lachrymal and salivary glands of the female rats showed massive infiltration of lymphocytes similar to the male pancreas (Fig. 1). Moreover, aged WBN/Kob rats (>18 months) showed thyroiditis, sclerotic cholangitis and even tubulointerstitial nephritis in both genders (Fig. 2). These findings suggest that WBN/Kob rats are an animal model for the LPSP type of AIP, showing extra-pancreatic sclerosing lesions without inflammatory bowel disease, but not the GEL type. Subsequently, analyses of the lymphocyte surface markers (Fig. 3), serum γ-globulin levels (Fig. 4), specific autoantibodies (Fig. 5) and the deposits of immune globulin (Fig. 6) showed that these lesions met the characteristics of autoimmune diseases defined by Witebsky and Mackay [29,30]. In addition to immunohistological findings, the prevention of pancreatitis and dacryoadenitis by the reconstitution of immune tolerance using BMT supports the correspondence as an autoimmune disease model (Fig. 7).

Human AIP involves both humoral immunity (autoantibody) and cell-mediated immunity (cytotoxic lymphocyte). We have reported previously that autoantibodies against

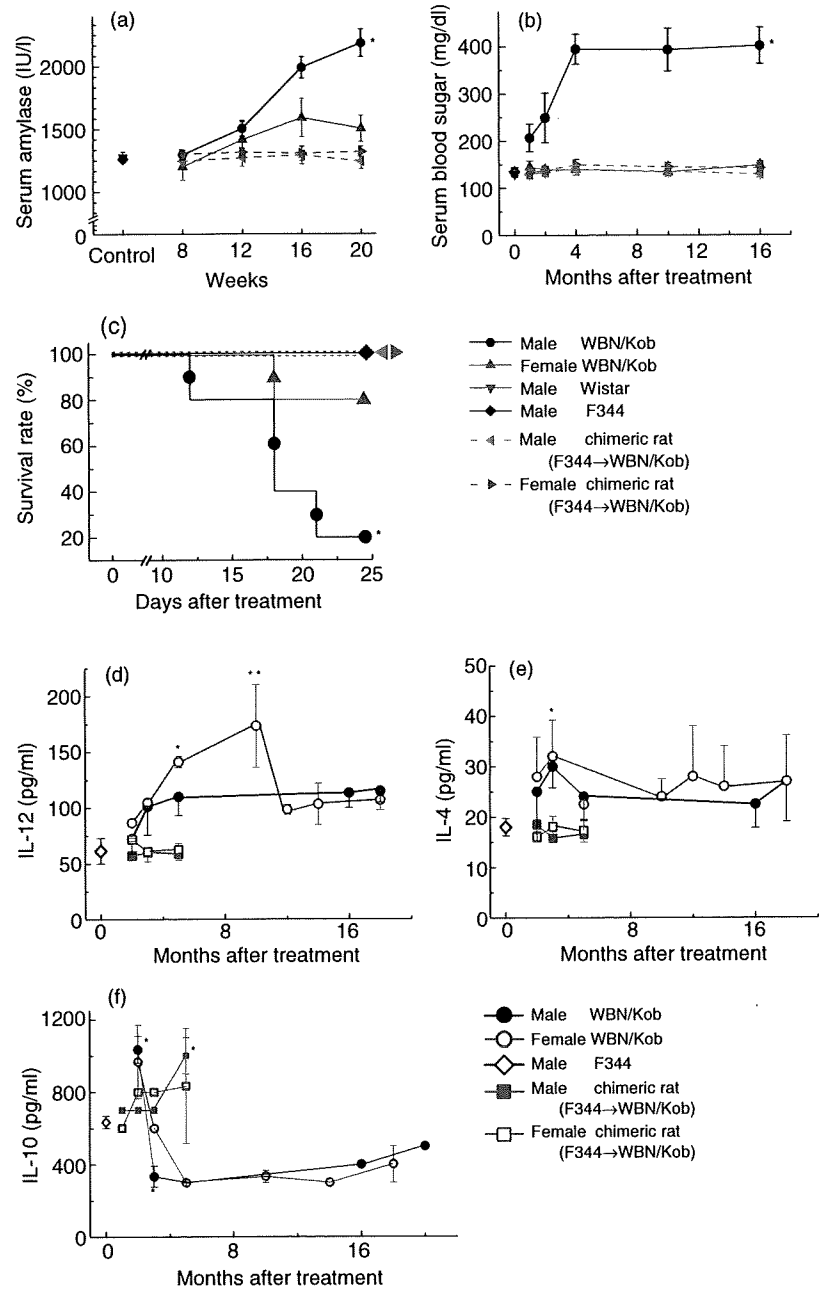

Fig. 9. Measurement of serum amylase, glucose, survival rate and cytokine levels. Serum amylase (a), glucose (b), survival rate (c), interleukin (IL)-12 (d), IL-4 (e) and IL-10 (f) were measured kinetically. Symbols and bars represent means ± standard deviations of seven rats. $^*P < 0{\cdot}05$.

CA-II and LF are identified frequently in patients with AIP, and that the prevalence of these two antibodies is independent [31]. Although the stage-dependent immunity in human AIP still remains unclear, T helper type 1/T helper type 2 (Th1/Th2) imbalance in the microenvironment is thought to reflect exacerbation progress. In fact, cytokine balance in the WBN/Kob rats suggested that Th2 cells are involved mainly in early development and Th1 cells are involved in progression, in comparison with the immunity of other AIP models that shifted into Th1 balance only because of artificial alloimmunization [18,19,32]. We also detected the specific autoantibodies of IgG2b type in WBN/Kob rats. Although details of the IgG subclass in rats remain unclear, rat IgG2b, a minor subclass of IgG, is separated in a similar position to human IgG4 by electrophoresis [33]. IgG2b subclass antibodies in the rats reflect the Th1/Th2 immune balance [34]. Up-regulation of the Th1 cytokine (interferon-γ) and down-regulation of IL-4 alter the Th1/Th2 balance to up-regulate IgG2b in the memory response, expand polyclonal activation and also expand the capacity of specific T helper cells. As reported previously, $CD4^+$ T cells react to CA-II or LF, which allows them to escape from negative selection in the thymus and depletion of T_{regs} such as $CD4^+$ $CD25^+$ T cells in the periphery. Although we identified

the specific antibody belonging to the IgG2b subclass in WBN/Kob rats in the present study, the details of other targeting antigens still remain unclear. Further studies on target antigens are necessary.

Recently, great attention has been paid to relations between various autoimmune diseases and T_{regs}. T_{regs} control immunological self-tolerance in the periphery [35,36]. The regulatory function is not mediated via CTLA-4 and cannot be blocked by antibodies to IL-4, IL-10 or transforming growth factor-β [6,13]. It has been clarified that their transcriptional factor, FoxP3, is the master gene for differentiation and function of T_{regs} [36]. In mice, neonatal thymectomy (NTx) induces the escape of T cells from negative selection in the thymus and depletes T_{regs} in the periphery, which results in the failure of both humoral and cellular immunity. Therefore, the NTx BALB/c mice, which had been immunized with CA-II or lactoferrin, nude mice (in which spleen cells of NTx mice had been transferred) developed immune-mediated pancreatitis and exocrinopathy [37]. Similarly, the WBN/Kob rats showed decreased numbers of peripheral $CD4^+$ $CD25^+$ T cells and $FoxP3^+$ splenic cells as reported in other autoimmune disease patients or animal models [38,39]. Our results showed that reconstitution of immune tolerance using BMT recovered the numbers of peripheral $CD4^+$ $CD25^+$ T cells and $FoxP3^+$ splenic cells, which resulted in the prevention of exocrinopathy in WBN/Kob rats. However, it still remains unclear as to whether or not all autoimmune diseases can originate from the abnormalities of T_{regs}. In WBN/Kob rats, cytokine alteration indicates that Th2 cells are involved mainly in early development and Th1 cells are involved in later development. Although it still remains unclear as to why organ-specific inflammation in human AIP and WBN/Kob rats depends on gender difference, factors such as sex hormones and genetic diathesis might be involved.

New immune therapies, such as suppressive, supportive and anti-cytokine therapies, can help to maintain and induce the remission of various autoimmune diseases [40]. However, as serious problems such as side effects of immune suppression often occur, these are radical treatments. Recently, haematopoietic stem cell transplantation has shown therapeutic efficacy in various kinds of autoimmune diseases [41]. In the WBN/Kob rats, we succeeded finally in preventing the development of inflammation by the achievement of complete chimerism; direct injection of the donor BMCs into the bone marrow cavity (by IBM–BMT) reduced the donor bone marrow trapping in the lung or liver [42]. The increased size of the $CD4^+CD25^+$ population and the up-regulation of FoxP3 after IBM–BMT as a treatment for ongoing pancreatitis and dacryoadenitis provide important evidence for the involvement of T_{regs} in the process of tolerance observed after induced relapses. The efficacy of IBM–BMT is not only a transient immunosuppression but, as we demonstrated, multiple interconnected mechanisms of immunomodulation. These findings suggest that IBM–BMT therapy may be a promising treatment of AIP in humans, although some complications such as rejection and infection should be carefully monitored. Again, taken together the WBN/Kob rats represent a novel model for the study of AIP with autoimmune extrapancreatic exocrinopathy.

Acknowledgements

Supported by grants from the Haiteku Research Center, the Millennium programme, the Science Frontier programme and the 21st Century Center of Excellence programme of the Ministry of Education, Culture, Sports, Science and Technology; a grant-in-aid for scientific research [(B) 11470062] and grants-in-aid for scientific research on priority areas [(A) 10181225 and (A) 11162221]; research grants from Health and Labor Sciences (Research on Human Genome, Tissue Engineering, Food Biotechnology), Department of Transplantation for Regeneration Therapy (sponsored by Otsuka Pharmaceutical Company Ltd), Molecular Medical Science Institute, Otsuka Pharmaceutical Company Ltd, Japan Immunoresearch Laboratories Co. Ltd, and the Ministry of Culture and Science of Japan (C18590755); and by a health and labour science research grant on intractable diseases of the pancreas from the Japanese Ministry of Health, Labor and Welfare. We also thank Mr Hilary Eastwick-Field, Mr Brian O'Flaherty and Ms K. Ando for their help in the preparation of the manuscript.

References

1 Kawaguchi K, Koike M, Tsuruta K *et al.* Lymphoplasmacytic sclerosing pancreatitis with cholangitis: a variant of primary sclerosing cholangitis extensively involving pancreas. Hum Pathol 1991; **22**:387–95.

2 Etemad B, Whitcomb DC. Chronic pancreatitis: diagnosis, classification, and new genetic development. Gastroenterology 2001; **120**:682–707.

3 Kamisawa T, Tu Y, Egawa N *et al.* Involvement of pancreatic and bile ducts in autoimmune pancreatitis. World J Gastroenterol 2006; **12**:612–14.

4 Finkelberg DL, Sahani D, Deshpande V *et al.* Autoimmune pancreatitis. N Engl J Med 2006; **355**:2670–6.

5 Okazaki K, Chiba T. Autoimmune related pancreatitis. Gut 2002; **51**:1–4.

6 Zamboni G, Luttges J, Capelli P *et al.* Histopathological features of diagnostic and clinical relevance in autoimmune pancreatitis: a study on 53 resection specimens and 9 biopsy specimens. Virchows Arch 2004; **445**:552–63.

7 Kim K, Kim M, Song M *et al.* Autoimmune chronic pancreatitis. Am J Gastroenterol 2004; **99**:1605–16.

8 Mufti R, Williamson R. Experimental models of pancreatitis. Ann Acad Med Singapore 1999; **28**:133–40.

9 Sakaguchi Y, Kusafuka K, Inaba M *et al.* Establishment of animal models for three types of pancreatitis and analyses of regeneration mechanisms. Pancreas 2006; **33**:371–80.

10 Kanno H, Nose M, Itoh J *et al.* Spontaneous development of

pancreatitis in the MRL/Mp strain of mice in autoimmune mechanism. Clin Exp Immunol 1992; **89**:68–73.
11 Vallance B, Hewlett B, Snider D *et al.* T cell-mediated exocrine pancreatic damage in major histocompatibility complex class II-deficient mice. Gastroenterology 1998; **115**:978–87.
12 Mori Y, Yokoyama J, Nishimura M *et al.* Diabetic strain (WBN/Kob) of rat characterized by endocrine–exocrine pancreatic impairment due to distinct fibrosis. Pancreas 1990; **5**:452–9.
13 Ohashi K, Kim J, Hara H *et al.* WBN/Kob rats. A new spontaneously occurring model of chronic pancreatitis. Int J Pancreatol 1990; **6**:231–47.
14 Tago Y, Katsuta O, Tsuchitani M *et al.* Glomerular lesions in spontaneously occurring diabetic WBN/Kob rats. J Comp Pathol 1991; **104**:367–77.
15 Nakamura S, Yamada T, Hashimoto T *et al.* Estradiol alleviates acinar cell apoptosis and chronic pancreatitis in male Wistar Bonn/Kobori rats. Pancreas 2003; **26**:59–66.
16 Tsuji A, Nishikawa T, Mori M *et al.* Quantitative trait locus analysis for chronic pancreatitis and diabetes mellitus in the WBN/Kob rat. Genomics 2001; **74**:365–9.
17 Hashimoto T, Yamada T, Yokoi T *et al.* Apoptosis of acinar cells is involved in chronic pancreatitis in WBN/Kob rats: role of glucocorticoids. Pancreas 2000; **21**:296–304.
18 Zipris D. Evidence that Th1 lymphocytes predominate in islet inflammation and thyroiditis in the BioBreeding (BB) rat. J Autoimmun 1996; **9**:315–19.
19 Piccirillo CA, Tritt M, Sgouroudis E *et al.* Control of type 1 autoimmune diabetes by naturally occurring CD4+CD25+ regulatory T lymphocytes in neonatal NOD mice. Ann NY Acad Sci 2005; **1051**:72–87.
20 Ikehara S, Good RA, Nakamura T *et al.* Rationale for bone marrow transplantation in the treatment of autoimmune diseases. Proc Natl Acad Sci USA 1985; **82**:2483–7.
21 Ikehara S. Treatment of autoimmune diseases by hematopoietic stem cell transplantation. Exp Hematol 2001; **29**:661–9. Review.
22 Kushida T, Inaba M, Hisha H *et al.* Intra-bone marrow injection of allogeneic bone marrow cells: a powerful new strategy for treatment of intractable autoimmune diseases in MRL/lpr mice. Blood 2001; **97**:3292–9.
23 Ikehara S. A novel strategy for allogeneic stem cell transplantation: perfusion method plus intra-bone marrow injection of stem cells. Exp Hematol 2003; **31**:1142–6. Review.
24 Masuya M, Drake C, Fleming P *et al.* Hematopoietic origin of glomerular mesangial cells. Blood 2003; **101**:2215–18.
25 Takada K, Inaba M, Ichioka N *et al.* Treatment of senile osteoporosis in SAMP6 mice by intra-bone marrow injection of allogeneic bone marrow cells. Stem Cells 2006; **24**:399–405.
26 Adachi Y, Oyaizu H, Taketani S *et al.* Treatment and transfer of emphysema by a new bone marrow transplantation method from normal mice to Tsk mice and vice versa. Stem Cells 2006; **24**:2071–7.
27 Yamamoto M, Takahashi H, Ohara M *et al.* A new conceptualization for Mikulicz's disease as an IgG4-related plasmacytic disease. Mod Rheumatol 2006; **16**:335–40.
28 Tsubota K, Fujita H, Tsuzaka K *et al.* Mikulicz's disease and Sjøgren's syndrome. Invest Ophthalmol Vis Sci 2000; **41**:1666–73.
29 Witebsky E. Concept of autoimmune disease. Ann NY Acad Sci 1966; **26**:443–50.
30 Mackay IR. Autoimmune disease. Med J Aust 1969; **29**:696–9.
31 Okazaki K, Uchida K, Ohana M *et al.* Autoimmune-related pancreatitis is associated with autoantibodies and a Th1/Th2-type cellular immune response. Gastroenterology 2000; **118**:573–81.
32 Davidson T, Longnecker D, Hickey W. An experimental model of autoimmune pancreatitis in the rat. Am J Pathol 2005; **166**:729–36.
33 Aithal P, Breslin P, Gumustop B *et al.* High serum IgG4 concentrations in patients with aclerosing pancreatitis. N Engl J Med 2001; **345**:147–8.
34 Bowman M, Holt G. Selective enhancement of systemic Th1 immunity in immunologically immature rats with an orally administered bacterial extract. Infect Immun 2001; **69**:3719–27.
35 Sakaguchi S. Regulatory T cells: key controllers of immunologic self-tolerance. Cell 2000; **101**:455–8.
36 Fontenot D, Gavin A, Rudensky Y. Foxp3 programs the development and function of $CD4^+CD25^+$ regulatory T cells. Nat Immunol 2003; **4**:330–6.
37 Uchida K, Okazaki K, Nishi T *et al.* Experimental immune-mediated pancreatitis in neonatally thymectomized mice immunized with carbonic anhydrase II and lactoferrin. Lab Invest 2002; **82**:411–24.
38 Viglietta V, Baecher-Allan C, Weiner H *et al.* Loss of functional suppression by $CD4^+CD25^+$ regulatory T cells in patients with multiple sclerosis. J Exp Med 2004; **199**:971–9.
39 Maul J, Loddenkemper C, Mundt P *et al.* Peripheral and intestinal regulatory $CD4^+$ CD25(high) T cells in inflammatory bowel disease. Gastroenterology 2005; **128**:1868–78.
40 Skurkovich S, Skurkovich B. Anticytokine therapy, especially anti-interferon-gamma, as a pathogenetic treatment in TH-1 autoimmune diseases. Ann N Y Acad Sci 2005; **1051**:684–700.
41 Tyndall A, Saccardi R. Haematopoietic stem cell transplantation in the treatment of severe autoimmune disease: results from phase I/II studies, prospective randomized trials and future directions. Clin Exp Immunol 2005; **141**:1–9.
42 Ikehara S. Intra-bone marrow-bone marrow transplantation: a new strategy for treatment of stem cell disorders. Ann NY Acad Sci 2005; **1051**:626–34.

Clinical and Experimental Immunology ORIGINAL ARTICLE doi:10.1111/j.1365-2249.2008.03615.x

Prevention of graft-*versus*-host disease by intrabone marrow injection of donor T cells: involvement of bone marrow stromal cells

T. Miyake,*† M. Inaba,*‡ J. Fukui,*† Y. Ueda,*§ N. Hosaka,*‡ Y. Kamiyama† and S. Ikehara*‡

*First Department of Pathology, †Department of Surgery, ‡Regeneration Research Center for Intractable Diseases, and §Department of Orthopedic Surgery, Kansai Medical University, Osaka, Japan

Accepted for publication 17 January 2008
Correspondence: Susumu Ikehara, First Department of Pathology, Kansai Medical University, Fumizono-cho, Moriguchi City, Osaka 570-8506, Japan.
E-mail: ikehara@takii.kmu.ac.jp

Summary

We have developed a new and effective method for bone marrow transplantation (BMT): bone marrow cells (BMCs) are injected directly into the bone marrow (BM) cavity of recipient mice. The intrabone marrow injection of BMCs (IBM-BMT) greatly facilitates the engraftment of donor-derived cells, and IBM-BMT can attenuate graft-*versus*-host reaction (GVHR), in contrast to conventional intravenous BMT (i.v.-BMT). Here, we examine the mechanisms underlying the inhibitory effects of IBM-BMT on GVHR using animal models where GVHR is elicited. Recipient mice (C57BL/6) were irradiated and splenic T cells (as donor lymphocyte infusion: DLI) from major histocompatibility complex-disparate donors (BALB/c) were injected directly into the BM cavity (IBM-DLI) or injected intravenously (i.v.-DLI) along with IBM-BMT. The BM stromal cells (BMSCs) from these recipients were collected and related cytokines were examined. The recipient mice that had been treated with IBM-BMT + i.v.-DLI showed severe graft-*versus*-host disease (GVHD), in contrast to those treated with IBM-BMT + IBM-DLI. The suppressive activity of BMSCs in this GVHD model was determined. The cultured BMSCs from the recipients treated with IBM-BMT + IBM-DLI suppressed the proliferation of responder T cells remarkably when compared with those from the recipients of IBM-BMT + i.v.-DLI in mixed leucocyte reaction. Furthermore, the level of transforming growth factor-β and hepatocyte growth factor in cultured BMSCs from IBM-BMT + IBM-DLI increased significantly when compared with those from the recipients of IBM-BMT + i.v.-DLI. Thus, the prevention of GVHD observed in the recipients of IBM-BMT + IBM-DLI was attributable to the increased production of immunosuppressive cytokines from BMSCs after interaction with host reactive T cells (in DLI).

Keywords: bone marrow stromal cells, donor lymphocyte infusion, graft-*versus*-host disease, intrabone marrow-bone marrow transplantation

Introduction

Allogeneic bone marrow transplantation (BMT) has been used as a potentially curative therapy for patients with a wide variety of diseases, including haematological disorders, congenital immunodeficiencies, metabolic disorders, autoimmune diseases and solid tumours [1–6]. However, there are several problems to be resolved in allogeneic BMT. One of the important issues is how to control graft-*versus*-host disease (GVHD), which remains a major cause of post-transplantation morbidity and mortality.

We have recently developed intrabone marrow (IBM)-BMT, in which bone marrow cells (BMCs) are injected directly into the bone marrow (BM) cavity [7]. We have found that IBM-BMT allows us not only to use low-dose irradiation as a preconditioning regimen [7,8] but also to suppress GVHD [9], as IBM-BMT can efficiently recruit donor-derived stromal cells [including mesenchymal stem cells (MSCs)] that can support donor-derived haemopoietic stem cells [1,9–12].

It is noted that IBM-BMT can be used to prevent GVHD, even when intensive donor lymphocyte infusion (DLI) is

carried out [9]. We attempted to inject allogeneic T cells as DLI into the BM cavity (IBM-DLI) or intravenously (i.v.-DLI) with IBM-BMT. The prolongation of survival rate and reduction of GVHD were observed clearly in the recipients treated with IBM-BMT + IBM-DLI, but not in those with IBM-BMT + i.v.-DLI [13]. These findings prompted us to examine the regulatory function of BM stromal cells (BMSCs) after interaction with T cells that had been injected into the BM cavity. Evidence has been accumulated that BMSCs play a critical role in the regulation of haemopoiesis by promoting cell-to-cell interactions and constitutively secreting immunoregulatory soluble factors [14–23]. In fact, BMSCs suppress the proliferation of allogeneic T cells in a major histocompatibility complex (MHC)-independent manner [24–31].

In the present study, we examine the suppressive activity of BMSCs that had been in contact with T cells *in vivo*, and evaluate the effect of T cell polarization and several factors produced by BMSCs.

Materials and methods

Mice

C57BL/6 (B6, H-2^b), BALB/c (H-2^d) mice were purchased from Shimizu Laboratory Supplies (Kyoto, Japan). C57BL/6 mice at the age of 7–9 weeks were used as recipients, and BALB/c mice at the age of 7–9 weeks were used as donors. All mice were kept in our animal facilities under specific pathogen-free conditions. All animal procedures were performed in accordance with protocols approved by the Animal Experimentation Committee, Kansai Medical University.

Irradiation

C57BL/6 mice were irradiated at 8·5 Gy (1·0 Gy/min) from a ^{137}Cs source (Gammacell 40 Exactor, Nordion, International Inc., Ottawa, Ontario, Canada) 1 day before the BMT.

Bone marrow transplantation and donor lymphocyte infusion

Bone marrow cells were flushed from the femoral and tibial bones of the BALB/c mice, and then suspended in RPMI-1640. The BMCs were then filtered through a 70-μm nylon mesh (Becton Dickinson Labware, Franklin Lakes, NJ, USA) to remove debris, washed and adjusted to $1{\cdot}5 \times 10^9$ cells/ml in RPMI-1640. The BMCs, thus prepared, were injected directly into the BM cavity as described previously [7]. Briefly, the region from the inguen to the knee joint was shaved and a 5-mm incision was made on the thigh. The knee was flexed to 90 degrees and the proximal side of the tibia was drawn to the anterior. A 26-gauge needle was inserted into the joint surface of the tibia through the patellar tendon and then inserted into the BM cavity. Using a microsyringe (10 μl; Hamilton Co., Reno, NV, USA) containing the donor BMCs ($1{\cdot}5 \times 10^9$ cells/ml), the donor BMCs were injected from the said bone holes into the BM cavity of the left tibia (10^7 cells/7 μl/tibia) (IBM-BMT). In some groups, BMCs were injected intravenously.

T cells were purified from the spleens by positive selection by a MACS® system using CD4 and CD8α microbeads (Miltenyi Biotec GmbH, Bergisch Gladbach, Germany) after depletion of red blood cells, or by an EPICS ALTRA flow cytometer (Coulter, Hialeah, FL, USA) after staining with fluorescein isothiocyanate (FITC)- or phycoerythrin (PE)-conjugated anti-CD4/CD8 monoclonal antibodies (mAbs) (BD Pharmingen, San Diego, CA, USA).

Splenic T cells were injected into the BM cavity of the right tibia (10^7 cells/7 μl/tibia: intrabone marrow T cell injection as DLI; IBM-DLI) or injected intravenously (i.v.-DLI; 10^7 cells/0·5 ml) into the recipient mice along with the IBM-BMT. Recipients treated with IBM-BMT alone (without DLI) served as negative controls (termed NO-DLI) [13].

Preparation of freshly isolated BMSCs

Three days after the DLI, BMCs were flushed from the right tibial bones of the recipient mice, and non-haemopoietic MSC-enriched cells (defined as $CD45^-/CD106^+$ cells) were sorted immediately by an EPICS ALTRA flow cytometer (Coulter, Hialeah, FL, USA) after staining with FITC- or PE-conjugated anti-CD45/CD106 mAbs (BD Pharmingen, San Diego, CA, USA). Freshly isolated non-haemopoietic BMSCs-enriched populations, sorted as $CD45^-/CD106^+$ cells, were prepared from the recipients of IBM-BMT + IBM-DLI, IBM-BMT + i.v.-DLI, or IBM-BMT alone (NO-DLI). Haemopoietic BMC-enriched populations, sorted as $CD45^+/CD106^-$ cells, were also prepared from the recipients and used as controls.

Preparation of cultured BMSCs

Bone marrow cells from the right tibia, into which T cells had been injected as DLI, were collected from the recipients of IBM-BMT + IBM-DLI, IBM-BMT + i.v.-DLI or IBM-BMT alone (without DLI) 3 days after treatment, and cultured in Dulbecco's modified Eagle's medium (DMEM) with 10% fetal calf serum (FCS). Two days later, non-adherent cells were removed. Adherent cells were detached using trypsin-ethylenediamine tetraacetic acid, and passaged when 80% confluence was reached and then replated. After 2 weeks (short-term culture) or 3 months (long-term culture) the cultures were discontinued, and BMSCs were harvested and used for further experiments, including mixed leucocyte reaction (MLR) and real-time reverse transcription–polymerase chain reaction (RT–PCR) assay. The culture-expanded BMSCs from the recipients of IBM-BMT +

